

# Adsorption of Phosphate in Aqueous Phase by Biochar Prepared from Sheep Manure and Modified by Oyster Shells

Yiyang Feng, Di Zhao, Shangkai Qiu, Qiuping He, Yuan Luo, Keqiang Zhang, Shizhou Shen, and Feng Wang\*



Cite This: *ACS Omega* 2021, 6, 33046–33056



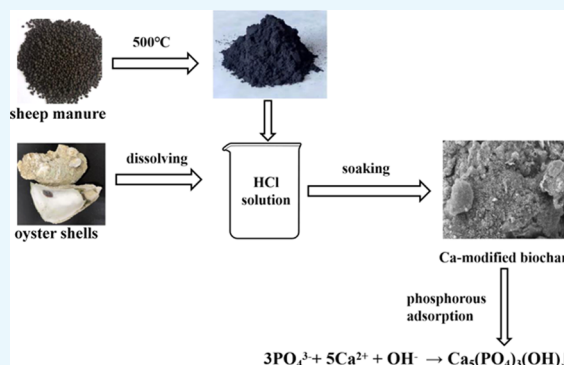
Read Online

ACCESS |

Metrics & More

Article Recommendations

**ABSTRACT:** Sheep manure and oyster shells as C and Ca sources, respectively, were used to obtain Ca-enriched biochar materials with a high dephosphorization efficiency. This approach is helpful for the utilization of livestock manure and shell solid waste as well as for creating highly adsorbent materials. The results show that as the Ca content in biochar was increased, the material's phosphate adsorption capacity increased. The maximum adsorption efficiency reached 94%. The highest adsorption capacity (calculated using Langmuir fitting) of the material containing 1:1 biochar/oyster shell weight ratio reached 146.3 mg P/g. With the increase of the pH value of phosphate solution, the adsorption capacity of the sample gradually increased to 89.5–93.3 mg P/g. The adsorption occurred mainly by complexation. The results of this work provide insights into livestock manure and shell solid waste utilization, which yields a material with useful adsorption properties that can be applied for the removal of phosphate and other inorganics from water.



## 1. INTRODUCTION

China is a large agricultural country with livestock and poultry industries as one of the most important sections, as they provide food for the population as well as advance China's economic development.<sup>1,2</sup> In the past 50 years, China's livestock and poultry breeding modes were switched from local free-range to large-scale breeding.<sup>3</sup> The second national pollution survey indicated that 378 800 large-scale livestock and poultry farms currently exist in China. Thus, with such large-scale livestock and poultry industries as well as their rapid developments, contamination of the environment, including drinking water and agricultural soils, by manure becomes more noticeable and even severe.<sup>3</sup> In fact, it is considered one of the largest sources of agricultural nonpoint pollution.<sup>4</sup> Statistics from the Chinese Animal Husbandry Yearbook showed that the output of livestock and poultry manure in China reaches 3.8 billion tons, but the comprehensive utilization rate is less than 60%. The research shows that biochar and bioenergy production from the pyrolysis of agricultural residues is a very environmentally friendly waste management approach.<sup>5</sup> In fact, several studies reported breakthrough data related to the biochar production from manure.<sup>6–8</sup>

Biochar, a solid product obtained by biomass pyrolysis in O<sub>2</sub>-deficient conditions,<sup>9,10</sup> possesses surface area, porosity, and active functional groups, all of which provide the biochar with excellent adsorption properties,<sup>11–14</sup> especially for the removal of N and P from water.<sup>15–18</sup> However, the surface of

traditional biochar is usually negatively charged, which makes the adsorption ability of biochar to phosphate poor.<sup>19,20</sup> In some cases, weakly absorbed phosphate was reported to be released back into the environment.<sup>19,20</sup> Most biochar shows Levin ion exchange capacity in which cations from the water phase are adsorbed through ion interaction and then attract anions, binding them.<sup>21</sup> This mechanism, capable of recovering dissolved phosphate under mild conditions, attracts scientists and engineers because of its low cost and environmental friendliness.<sup>22–26</sup> The common phosphate adsorbents mainly include silicates, modified metals, and their oxides. Silicate adsorbents have wide sources and low prices but their adsorption capacity is limited.<sup>27,28</sup> Metal and metal-oxide adsorbents have high adsorption capacity and fast adsorption speed for phosphate, but they are easy to agglomerate, and excessive accumulation of most metals will cause toxicity.<sup>29,30</sup> Therefore, in contrast, the application of solid waste adsorption materials based on biochar can also alleviate the environmental pollution problem on the premise of ensuring

Received: September 18, 2021

Accepted: November 10, 2021

Published: November 23, 2021



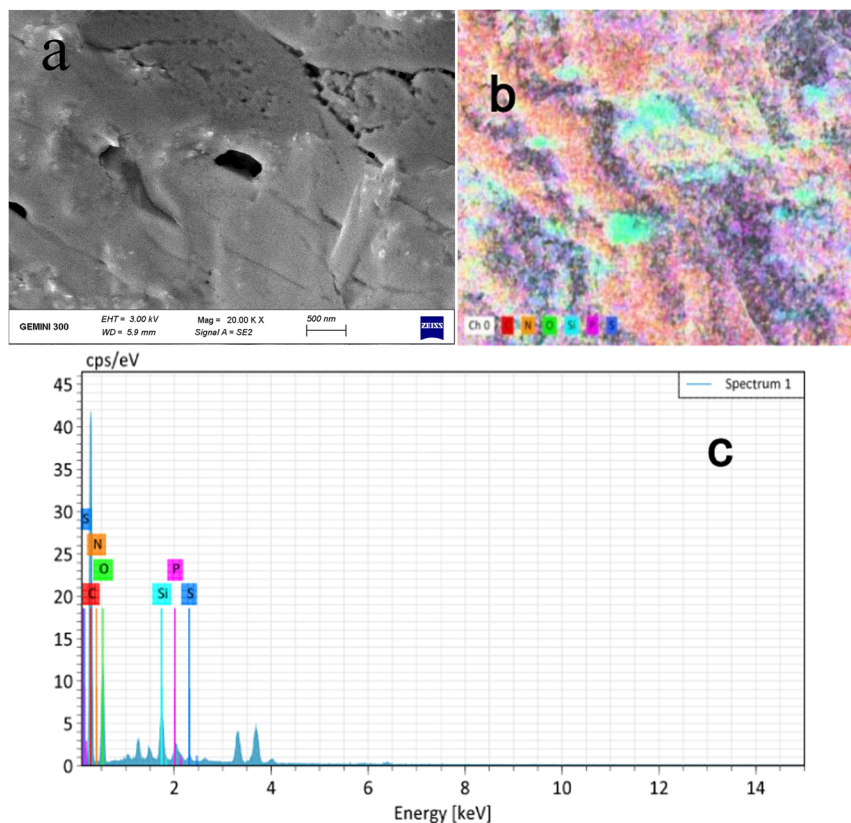


**Figure 1.** SEM (a) and EDS (elemental mapping (b) and a full spectrum (c)) data obtained for the unmodified biochar BC sample.

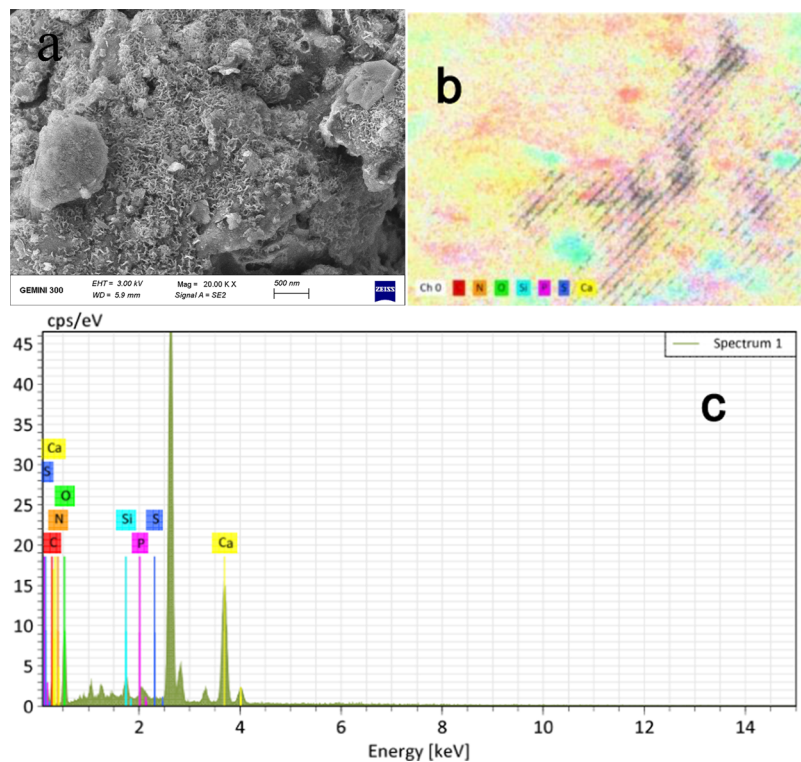


**Figure 2.** SEM (a) and EDS (elemental mapping (b) and a full spectrum (c)) data obtained for the modified biochar BC-5 sample.

the adsorption capacity and not producing secondary pollution, thus killing two birds with one stone.<sup>11–14</sup>

Biochar modification by Ca is also promising as this method does not generate any toxic waste or byproducts and is easy to

accomplish.<sup>31–34</sup> It has been reported that the adsorption capacity of calcium-modified biochar for phosphate in water is at a high level, ranging from 96.56 to 197 mg/g.<sup>32,35</sup> Typical biochar Ca-modification methods use Ca-containing chem-

**Table 1. Compositions of the Biochar, Oyster Shells, and Ca-Modified Biochar**

	C (%)	H (%)	O (%)	N (%)	S (%)	P (%)	Ca (%)	K (%)	Na (%)	Si (%)
sheep manure	25.47	4.65	30.21	1.68	0	0.31	0.59	0.2	0.10	0.68
oyster shell	12.14	0.22	38.83	0.14	0	0	38.28	0	0.61	0.07
BC	43.25	2.65	19.50	2.40	0	0.44	0.25	2.99	0.26	1.24
BC-5	44.6	4.36	38.64	0.83	0	0.21	7.72	0.37	0.18	0.24
BC-5 + P	40.57	2.50	16.72	1.72	0	3.84	7.69	0.08	0.04	0.32

icals, which increases the overall production cost and makes scaling up difficult.<sup>20,34,36,37</sup> Thus, researchers started looking for cost-effective raw materials.<sup>9,38,39</sup> Calcium, often bonded with carbon and its compounds, is abundant in natural materials, which are often discarded.<sup>17,31,32,35</sup> One example is oyster shells. The main component of oyster shells is calcium carbonate ( $\text{CaCO}_3$ ).<sup>40</sup> Results of the 2016 national pollution survey in China revealed that oyster cultures reached 4.83 million tons, which translates into tons of discarded oyster shells, occupying vast land resources and potentially threatening human health and the surrounding environments.<sup>41</sup> One way to utilize these discarded oyster shells is to use them as a Ca source to modify biochar.

Therefore, this work used sheep manure as a C source to prepare biochar with a high surface area. This biochar was then modified with Ca from the discarded oyster shells. The resulting materials were used to remove phosphate from the wastewater. The main objective of this study is to prepare biochar with waste as the raw material to achieve high adsorption capacity of phosphate in aqueous solutions. The results obtained in this work also provide new insights on how the waste materials (livestock and poultry manure as well as discarded oyster shells) can be utilized and reused for other useful purposes.

## 2. RESULTS AND DISCUSSION

### 2.1. Physical and Chemical Properties of Materials.

The biochar surface prior to modification was smooth with some irregular protrusions according to the scanning electron microscopy (SEM) results shown in Figure 1. After the modification with oyster shells, the surface became grainier and flaky with some rod-like features (see Figure 2). The results are similar to those of some metal-loaded biochar by SEM. Through some modification methods, metals can be loaded on the surface of biochar in the form of particles or rods.<sup>39,42</sup> Comparison of energy-dispersive spectra (EDS) of unmodified biochar and BC-5 samples clearly indicated the presence of Ca in the modified sample (see Figures 1c and 2c, respectively). Thus, a Ca-enriched biochar composite material was successfully obtained.

The initial Ca content in the oyster shells was 38.3%. Combining these results with O and C contents (shown in Table 1) confirms that the oyster shells primarily consisted of  $\text{CaCO}_3$ .<sup>40</sup> The Ca content in the BC-5 sample was 7.72%. It remained almost the same (7.69%) after the modified biochar was used for P adsorption experiments, indicating the excellent stability of the composite materials. After BC-5 adsorbed phosphate, the P content increased from 0.21 to 3.84%, which proved that BC-5 had a good phosphate adsorption effect. Some studies have also shown that metals such as calcium are positively correlated with the adsorption of phosphate by biochar.<sup>31</sup>

The surface area as well as pore volume and diameters of biochar increased after carbonization and then decreased after

enrichment with Ca (see Table 2). The surface area is an important factor that controls the adsorption performance.<sup>31</sup>

**Table 2. Surface Area, Pore Volume, and Pore Diameters of Biochar Before and After Enrichment with Ca**

	$S_{\text{BET}}$ ( $\text{m}^2/\text{g}$ )	pore volume ( $\text{cm}^3/\text{g}$ )	pore size (nm)
sheep manure	2.2603	0.0078	13.8299
BC	5.1364	0.0157	18.2016
BC-5	4.7357	0.0139	10.1599

The organic carbon in the original biomass may be largely removed during pyrolysis, resulting in higher pore volume and pore size, which is consistent with the previous research conclusions.<sup>31,34,43</sup> Thus, the material became denser after Ca was introduced. We also believe that the biochar surface was modified by the hydroxyapatite ( $\text{CaCl}_2(\text{H}_2\text{O})_6$ )<sup>44</sup> (which was detected by X-ray diffraction (XRD), as discussed below), which also contributed to the surface area and porosity decrease. This is because  $\text{CaCl}_2(\text{H}_2\text{O})_6$  blocked the micro-porous structure of biochar.<sup>39</sup>

### 2.2. Fourier Transform Infrared (FTIR) spectroscopy and XRD.

FTIR spectra of BC and BC-5 (before and after adsorption experiments) showed peaks at 3419 and 1626  $\text{cm}^{-1}$  (see Figure 3a)<sup>31,45</sup> belonging to  $-\text{OH}$  and  $-\text{CH}_2-$  vibrations, respectively. The asymmetric tensile P–O vibrations of  $\text{H}_2\text{PO}_4^-$  and  $\text{HPO}_4^{2-}$  groups in biochar, detected at 1041  $\text{cm}^{-1}$ ,<sup>42,44</sup> weakened after the biochar was modified with oyster shells but became stronger after the modified biochar was used for P adsorption experiments. The FTIR spectra of BC-5 + P showed peaks at 601 and 564  $\text{cm}^{-1}$  corresponding to the symmetric O–P–O vibrations of the  $\text{PO}_4^{3-}$  group.<sup>43</sup> Thus, FTIR spectra confirmed inductively coupled plasma optical emission spectrometry (ICP-OES) results as well as successful adsorption of phosphate by the modified biochar.

The XRD spectrum of unmodified biochar showed only  $\text{SiO}_2$  peaks according to the PDF card number 85-0798 (see Figure 3b). The XRD spectrum of BC-5 showed that the main form of Ca was  $\text{CaCl}_2(\text{H}_2\text{O})_6$  (according to the PDF card number 77-1782), which formed after oyster shells were dissolved by HCl and redeposited on the biochar surface. Ca in the BC-5 sample subjected to the phosphate adsorption tests (sample marked as BC-5 + P) was mainly in the  $\text{Ca}_5(\text{PO}_4)_3(\text{OH})$  form according to the XRD peaks matching PDF card number 09-0432. Thus,  $\text{PO}_4^{3-}$  was complexed by biochar's  $\text{Ca}^{2+}$  yielding hydroxyapatite. These results confirmed the literature reports, which used chemical reagents as Ca sources.<sup>9,20,34,36,37</sup>

**2.3. Effect of the Initial Biochar: Shell Ratios on the Adsorption Capacity of the Ca-Enriched Biochar.** As the amount of oyster shell powder used to treat biochar was increased, the adsorption capacity of the Ca-enriched biochar toward phosphate also increased (see Figure 4). When 5 mg/L phosphate was present in the solution, the adsorption

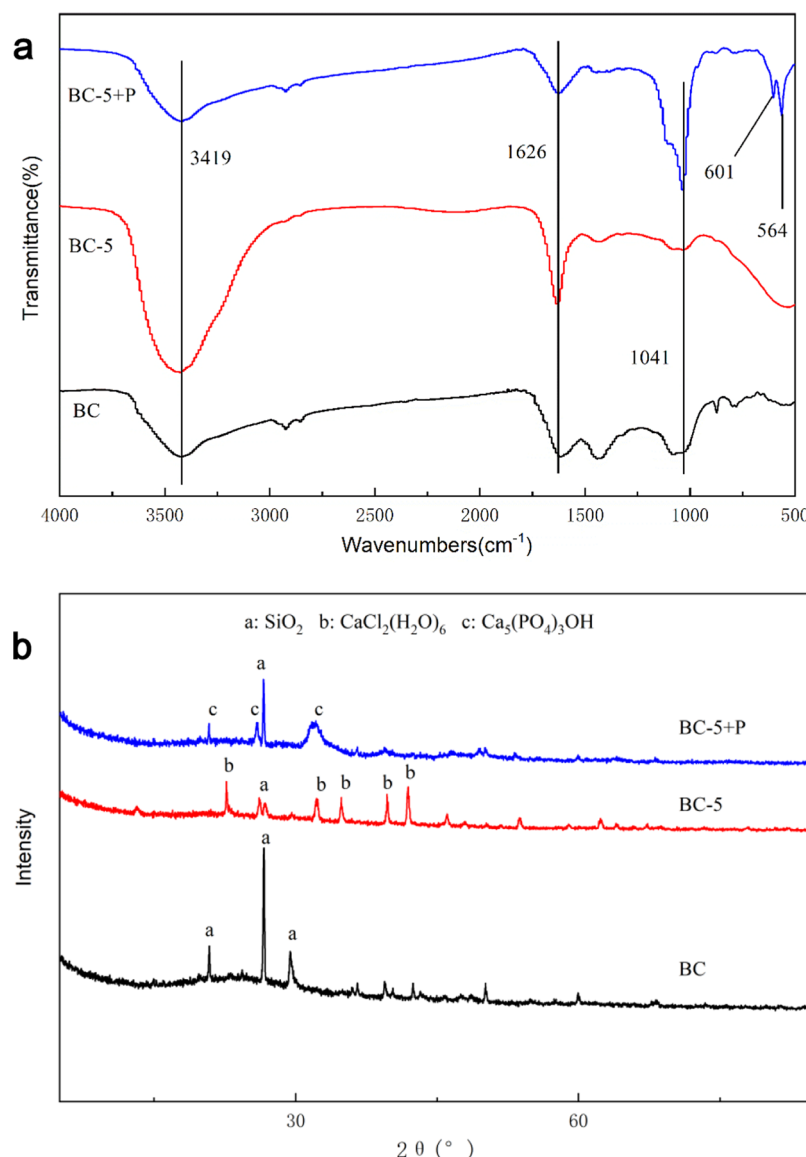


**Figure 3.** FTIR (a) and XRD (b) patterns of BC, BC-5, and BC-5 + P samples.

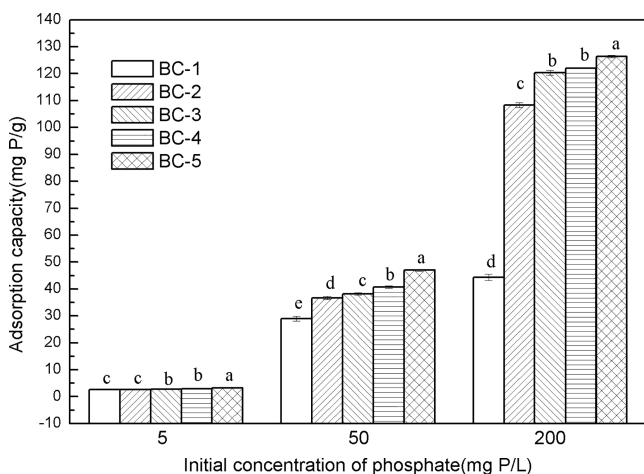


**Figure 4.** Comparison of adsorption efficiency of the Ca-enriched biochar samples at different phosphate concentrations. Note: lower-case letters of phosphate concentration in each group indicate a significant difference between the datasets ( $P < 0.05$ ).

capacities of our samples were equal to 2.56–3.19 mg P/g. At this concentration, BC-5 composite demonstrated the highest efficiency, equal to 63.83%. At 50 mg P/L, our composite biochar samples' adsorption capacities were in the 28.92–47.00 mg P/g range. At the same time, the adsorption efficiency of the BC-5 sample was the highest and equal to 94.00%. When 200 mg/L phosphate was present, the adsorption capacities of the Ca-enriched biochar samples were in the 44.33–126.33 mg P/g range. The adsorption efficiency of the BC-5 sample was again the highest and equal to 63.17%.

According to the significant difference analysis results of SPSS software, no significant differences in adsorption capacity between BC-1 and BC-2 and between BC-3 and BC-4 material samples were observed at phosphate concentration equal to 5 mg P/L. However, significant differences in adsorption capacity were observed between BC-5 and other samples. When 50 mg P/L was present in the experimental solution, the adsorption capacities of all samples differed significantly. However, when the solutions contained 200 mg P/L, the adsorption capacities of BC-1 and BC-2 were significantly

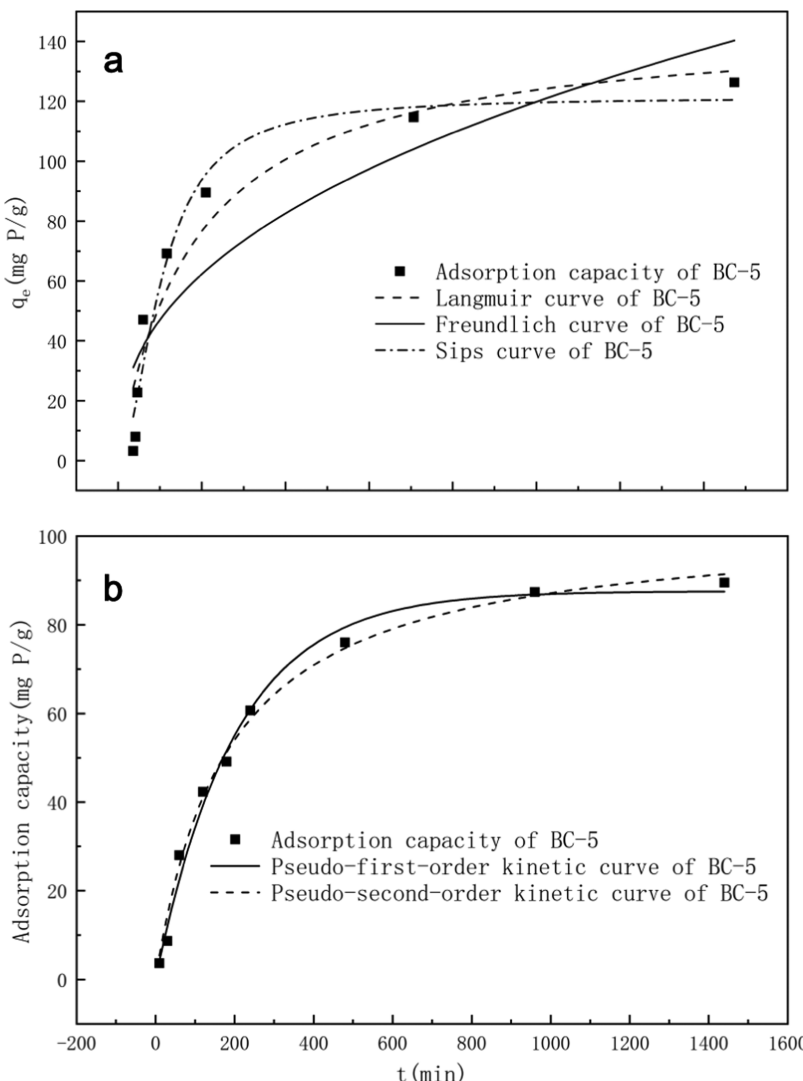


**Figure 5.** Isotherm (a) and kinetic (b) curves of phosphate adsorption on BC-5.

different, but those of BC-3 and BC-4 were insignificantly different. At this concentration, the adsorption capacity of BC-5 was significantly different from other samples. Thus, as more oyster shell powder was added to the biochar, the adsorption performance improved.

The initial form of Ca in BC-5 was  $\text{CaCl}_2(\text{H}_2\text{O})_6$ , which reacted with  $\text{PO}_4^{3-}$  from the solution forming hydroxyapatite.<sup>9</sup> Studies of Ca-enriched adsorbents, including sepiolite, carbonate montmorillonite,<sup>47</sup> natural clinoptilolite treated with  $\text{Ca}(\text{OH})_2$ ,<sup>48</sup> activated zeolite,<sup>49</sup> and attapulgite,<sup>50</sup> reported that the presence of Ca significantly enhanced the matrix adsorption capacity. The adsorption mechanisms of these Ca-modified materials were based on the ligand exchange between  $\text{Ca}^{2+}$  and phosphate near the biochar surface, followed by surface precipitation.<sup>46–50</sup> All characterization results discussed above indicated that the presence of Ca was the primary factor contributing to the enhanced phosphate adsorption by the biochar. It was especially noticeable for the samples with high oyster shell contents. The primary phosphate adsorption mechanism was chemical adsorption coupled with complexation.

**2.4. Phosphorus Adsorption Isotherms.** Phosphate adsorption isotherm for the BC-5 composite showed that the

amount of the total adsorbed P positively correlated with the equilibrium phosphate concentration (see Figure 5a). The best fit of our adsorption data was obtained using the Langmuir equation (see Table 3): the correlation coefficient  $R^2$  was equal to 0.91. The shape of the isotherm indicated that phosphate was adsorbed uniformly on BC-5 and that no interaction

**Table 3. Fitting Parameters Obtained from Phosphate Adsorption (on BC-5) Isotherms by Applying Langmuir, Freundlich, and Sips models Obtained Using BC-C5 Adsorbent**

isotherm models	parameters	
Langmuir	$q_{\max}$ (mg P/g)	146.28
	$K_L$	0.11
	$R^2$	0.91
Freundlich	$K_F$	24.43
	$1/n$	0.41
	$R^2$	0.78
Sips	$q_{\max}$ (mg P/g)	121.29
	$K_s$	0.045
	$n_s$	0.53
	$R^2$	0.95

between phosphate anions existed. This data agrees with the literature reports on the monolayer phosphate adsorption<sup>9,26,43,45,S1,S2</sup> as well as with our results, which showed that phosphate adsorption by Ca-enriched biochar occurred through the  $\text{Ca}^{2+}$  reaction with  $\text{PO}_4^{3-}$ .<sup>99</sup> The maximum adsorption capacity obtained from Langmuir fitting was equal to 146.28 mg P/g. This value falls in the middle of the literature values obtained for the biochar modified with Ca-containing chemicals (see Table 4). Typically,  $1/n$  slope

**Table 4.** Adsorption Capacities of Various Ca-Modified Biochar from the Literature and This Work

raw materials	origin of Ca	$q_{\max}$ (mg P/g)	references
straw biochar	$\text{Ca(OH)}_2$	197	36
sludge biochar	$\text{CaCl}_2$	168.70	38
clay biochar	$\text{Ca(OH)}_2$	147.0588	34
sheep manure biochar	oyster shell	146.33	this study
ramie biochar	$\text{CaCl}_2$	105.406	43
rape pollen biochar	$\text{CaCO}_3$	96.56	32

obtained from the Freundlich equation is used as an index of how difficult the adsorption reaction proceeds:<sup>46</sup> if  $1/n$  is in the 0.1–0.5 range, it is relatively easy for the phosphate to be adsorbed, while at  $1/n > 2$ , the adsorption is considered problematic. Our  $1/n$  value obtained for phosphate adsorption by BC-5 was equal to 0.41. Thus, this adsorption process was favorable. The highest fitting accuracy was obtained when we fitted our adsorption data using the Sips model, which implies that phosphate adsorption on the BC-5 surface was a combination of mono- and multilayer adsorption.<sup>32</sup>

**2.5. Kinetics of Phosphate Adsorption on the Ca-Modified Biochar.** As the phosphate adsorption time on BC-5 was increased, the adsorption capacity first increased rapidly (during the first 200 min) and then stabilized at 200–400 min (see Figure 5b) because the active biochar sites became gradually occupied. The adsorption rate of BC-5 was faster than that of other kinds of biochar reported in previous publications.<sup>45</sup> This data was best fitted using the pseudo-second-order kinetic model (see Table 5), judging by the

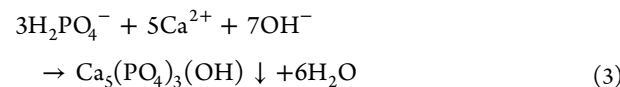
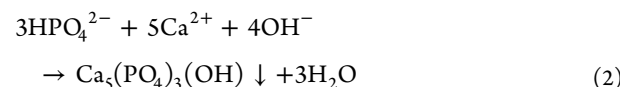
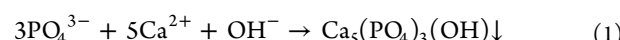
**Table 5.** Kinetic Parameters Obtained by Fitting the Experimentally Obtained Data of Phosphate Adsorption on the BC-5 Biochar

pseudo-first-order dynamic equation			pseudo-second-order dynamic equation		
$q_e$ (mg P/g)	$K_1$	$R^2$	$q_e$ (mg P/g)	$K_2$	$R^2$
87.55	0.005	0.9896	102.84	$5.39 \times 10^{-5}$	0.9915

corresponding fitting coefficient  $R^2 = 0.9901$ . Thus, the phosphate adsorption rate by BC-5 was controlled by the chemical adsorption mechanism, which agrees with the previous literature reports.<sup>9,14,17,39,45</sup> It is proved that the phosphorus removal process of BC-5 was mainly due to chemical bonding or chemisorption involving sharing electrons between phosphate ionic species and Ca-doped biochar.<sup>34</sup> The equilibrium adsorption capacity calculated from the pseudo-second-order kinetic equation was 87.55 mg P/g, which is very close to the value obtained experimentally (equal to 89.50 mg P/g).

**2.6. pH Influence on the BC-5 Phosphate Adsorption Capacity.** Phosphate adsorption on BC-5 gradually increased

with pH (see Figure 6a). At pH values below 7, the BC-5 capacity was 65 mg P/g, while above 7 it was 89.50–93.33 mg P/g. The highest adsorption efficiency (equal to 93.33%) was achieved at pH = 11. Thus, the most efficient phosphate adsorption by BC-5 occurred under strong alkaline conditions, while under acidic and neutral conditions, the adsorption was moderate. This is because, according to the following eqs 12–3, the main chemical reaction in the adsorption process is the formation of  $\text{Ca}_5(\text{PO}_4)_3(\text{OH})$  by  $\text{Ca}^{2+}$  and  $\text{PO}_4^{3-}$  under alkaline conditions.<sup>9</sup> This data shows the high pH adaptability of our Ca-enriched biochar toward phosphate adsorption. Adsorption of phosphate on Ca-containing biochar at different concentrations of  $\text{OH}^-$  can be described by the following reactions<sup>9</sup>



Thus,  $\text{Ca}^{2+}$  reaction with  $\text{PO}_4^{3-}$  will be hindered under acidic conditions, which agrees with the literature data on phosphate adsorption by the biochar modified with Ca-containing chemicals.<sup>20,34,36,37</sup>

**2.7. Interference of Phosphate Adsorption on Ca-Modified Biochar by other Anions.** Data on the phosphate adsorption interference by the presence of  $\text{Cl}^-$ ,  $\text{CO}_3^{2-}$ ,  $\text{HCO}_3^-$ ,  $\text{NO}_3^-$ , and  $\text{SO}_4^{2-}$  is shown in Figure 6b. When  $\text{CO}_3^{2-}$  and  $\text{HCO}_3^-$  were present, the BC-5 adsorption capacity increased by 4.28 and 1.31%, which are significant differences according to our statistical analysis performed considering the blank group without adding any coexisting ions (CK) and the group with  $\text{CO}_3^{2-}$  and  $\text{HCO}_3^-$ . At the same time,  $\text{Cl}^-$ ,  $\text{NO}_3^-$ , and  $\text{SO}_4^{2-}$  inhibited phosphate adsorption by the BC-5 material: the corresponding adsorption capacities decreased by 0.93, 3.72, and 2.79%. Statistical analysis showed no significant difference among the blank and  $\text{Cl}^-$ -containing groups. However, the blank group and the groups containing  $\text{NO}_3^-$  and  $\text{SO}_4^{2-}$  showed significant differences. But the adsorption capacity was still equal to 86.17 mg P/L.

$\text{Cl}^-$ ,  $\text{CO}_3^{2-}$ ,  $\text{HCO}_3^-$ ,  $\text{NO}_3^-$ ,  $\text{SO}_4^{2-}$ , and  $\text{PO}_4^{3-}$  often coexist in natural waters. These ions might create an anionic environment around the active biochar surface sites, which could weaken its electrostatic interactions with  $\text{PO}_4^{3-}$ .<sup>51,53</sup> Additionally, these anions might compete with  $\text{PO}_4^{3-}$  for these sites,<sup>37,S1,S3,S4</sup> which was the case when we added  $\text{NO}_3^-$  and  $\text{SO}_4^{2-}$  to the solutions containing BC-5 and phosphate: the BC-5 adsorption capacity decreased.<sup>25</sup> However, the addition of the weakly acidic  $\text{CO}_3^{2-}$  and  $\text{HCO}_3^-$  anions increased the pH (from 8.0 to 9.13). According to our results, higher pH values are beneficial for the facilitated  $\text{PO}_4^{3-}$  reaction with Ca in BC-5, so the adsorption capacity increased.

### 3. CONCLUSIONS

This work reports preparation of Ca-modified biochar using oyster shells and sheep manure as raw materials. The resulting Ca-rich composite material was then tested for phosphate adsorption. Phosphate adsorption capacity of the Ca-enriched biochar was 146.33 mg P/g, which is very comparable to the

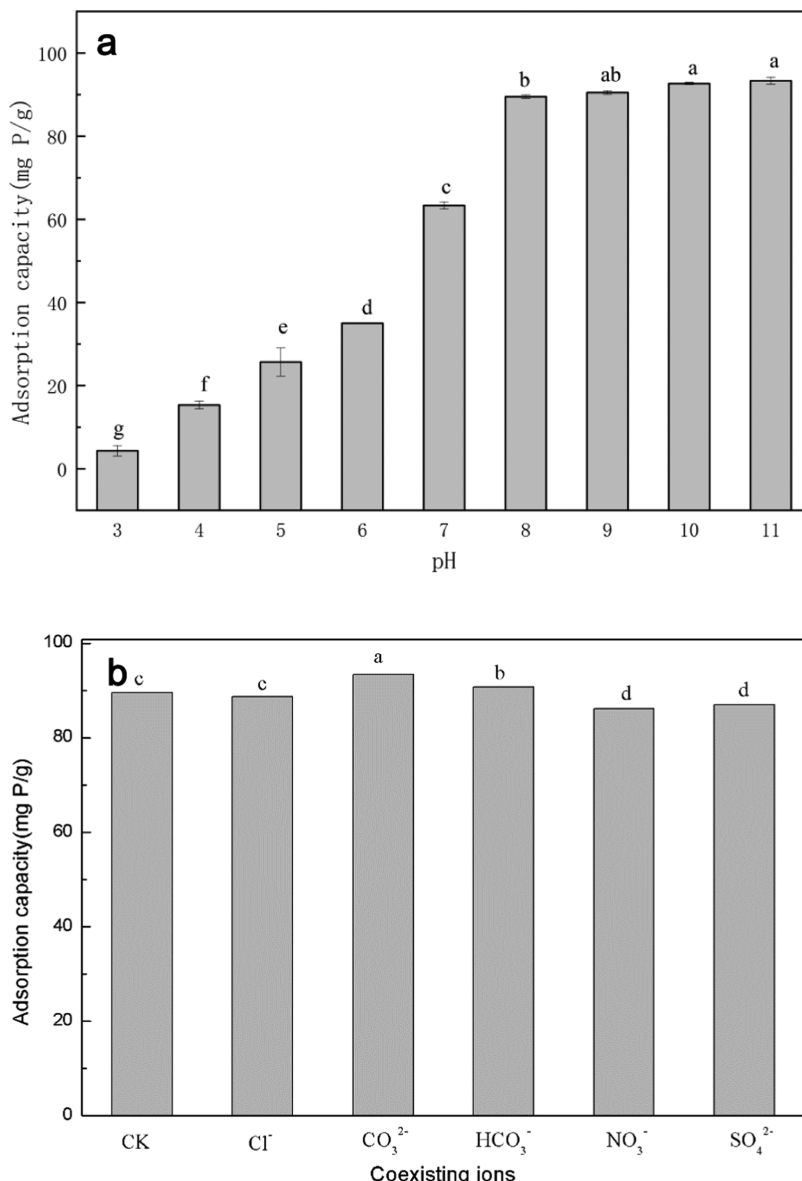


**Figure 6.** BC-5 adsorption capacity toward phosphate as a function of pH (a) and coexisting ions (b). Note: each lowercase letter indicates a significant difference between the datasets ( $P < 0.05$ ).

capacities of the biochar modified with Ca-containing chemicals. The experimental data obtained for phosphate adsorption by the Ca-enriched biochar was fitted by the Langmuir and quasi-second-order kinetic models. Phosphate adsorption by Ca-modified biochar could be described as the chemical monolayer adsorption. At pH values below 7, the adsorbing capacity of the Ca-modified biochar was below 65 mg P/g. However, at pH above 7, the adsorption capacity was in the 89.50–93.33 mg P/g range. Thus, phosphate adsorption on our Ca-enriched biochar could occur over a wide pH range. FTIR and XRD data suggested that phosphate adsorption by the Ca-enriched biochar occurred through phosphate complexation. Thus, treating pyrolyzed manure with natural Ca-rich oyster shells is an effective way to obtain well-adsorbing materials and utilize solid waste. Moreover, this study can provide theoretical basis for the improvement of the preparation process of calcium-modified biochar and its phosphate adsorption mechanism.

#### 4. EXPERIMENTAL SECTION

**4.1. Materials.** The manure from the black short-haired sheep and oyster shells from the Beihai oyster were collected from the Dali Prefecture of Yunnan Province and the Beihai City (Guangxi Zhuang Autonomous Region), respectively. After the collection, the shells and manure were dried in the sun, ground, and passed through 60- and 20-mesh sieves, respectively. The experiments show that oyster shells can be dissolved in hydrochloric acid more quickly after passing through a 60-mesh sieve, and sheep manure can be heated evenly during pyrolysis after passing through a 20-mesh sieve.

**4.2. Biochar Preparation.** All experiments were carried out in Dali Agricultural Environmental Science Observation and Experimental Station at the Ministry of Agriculture and Rural Affairs. The screened manure was placed in a crucible and heated up to 500 °C with a heating rate of 5 °C/min and a holding time of 2 h under N<sub>2</sub> atmosphere. The obtained biochar samples were ground and passed through a 60-mesh sieve. Then, 10 g of the powder was mixed with 1 L of

deionized water, stirred, and allowed to stand still for 30 min. The solution was then passed through a 0.45  $\mu\text{m}$  filter. The filtered biochar was rinsed three times with water and dried at 105 °C until no weight changes were observed. The biochar was named BC.

Several samples with the biochar:shell mass ratios equal to 1:0.1, 1:0.3, 1:0.5, 1:0.7, and 1:1 were prepared and marked as BC-1, BC-2, BC-3, BC-4, and BC-5, respectively. For this purpose, 10 g of the biochar was mixed with the corresponding volumes of 0.01 g/mL oyster shell solution (oyster shells were dissolved in 2 mol/L HCl solution). The resulting mixtures were allowed to stand for 24 h after which they were dried at 105 °C until no weight changes were registered.

**4.3. Adsorption Tests.** An amount of 0.05 g of the Ca-enriched biochar was placed into a 100 mL flask after which 50 mL of KH<sub>2</sub>PO<sub>4</sub> solution was added (phosphate concentration used in different experiments is different, which has been discussed in Sections 4.4, 4.5, 4.6, and 4.7). The mixture was then placed for 24 h in a constant-temperature (25 ± 0.5 °C) oscillating incubator rotating at 180 rpm, after which the supernatant was passed through a 0.45  $\mu\text{m}$  filter. The phosphorus content in the supernatant was obtained using a double beam UV-visible spectrophotometer manufactured by TU-1901 Beijing General Instrument Corporation (using the molybdate method). Adsorption experiments for each sample were repeated here three times using a new material every time. All of the adsorption data reported in this paper represent the average of these three measurements. The equilibrium adsorption capacity ( $q_e$ ) was calculated as shown below

$$q_e \text{ (in mg P/g)} = \frac{(C_0 - C_e)V}{m} \quad (4)$$

where  $C_0$  and  $C_e$  are the initial and equilibrium phosphorus concentrations (in mg P/L), respectively;  $V$  is the solution volume (in L); and  $m$  is the adsorbent weight (in g).

Samples subjected to phosphate adsorption experiments were marked with “+P” (e.g., BC-5 + P). The statistical analysis of the adsorption data was performed using SPSS26.0 software with a 0.05 significance level.

**4.4. Phosphate Adsorption by the Composite Biochar at Different pH Values.** An amount of 0.05 g of the BC-5 sample was mixed with 50 mL of 100 mg P/L KH<sub>2</sub>PO<sub>4</sub> solution with pH values equal to 3–11 (±0.05). The adsorption process and phosphate determination method are the same as those in Section 4.3.

**4.5. Isothermal Adsorption Experiments.** An amount of 0.05 g of BC-5 (the experiments show that BC-5 has the best performance in phosphate adsorption) sample was mixed with 50 mL of KH<sub>2</sub>PO<sub>4</sub> solution with pH = 8, the total phosphorus contents of which were equal to 5, 10, 25, 50, 75, 100, 150, and 200 mg P/L. The adsorption process and phosphate determination method are the same as those in Section 4.3.

The experimental data were fitted by the Langmuir, Freundlich, and Sips equations shown below<sup>32,34</sup>

$$\text{Langmuir: } q_e = q_{\max} \frac{K_L C_e}{1 + K_L C_e} \quad (5)$$

$$\text{Freundlich: } q_e = K_F C_e^{1/n} \quad (6)$$

$$\text{Sips: } q_e = q_{\max} \frac{K_s C_e^{1/n_s}}{1 + K_s C_e^{1/n_s}} \quad (7)$$

where  $q_e$  and  $q_{\max}$  are the equilibrium and maximum adsorption capacities (in mg P/g), respectively;  $C_e$  is the equilibrium P concentration (in mg P/L);  $K_L$ ,  $K_F$ , and  $K_s$  are the adsorption affinity parameters; and  $n$  and  $n_s$  are nonlinear coefficients.

**4.6. Kinetic Adsorption Experiments.** An amount of 0.05 g of the BC-5 sample was placed into a 100 mL flask after which 50 mL of 100 mg P/L KH<sub>2</sub>PO<sub>4</sub> solution with pH = 8 was added. The resulting mixtures were then shaken at 180 rpm at 25 ± 0.5 °C for 10, 30, 60, 120, 180, 240, 480, 720, and 1440 min. The adsorption process and phosphate determination method are the same as those in Section 4.3.

All experimentally obtained data were treated by the pseudo-first- and pseudo-second-order kinetic models,<sup>32,39</sup> shown in eqs 8 and 9, respectively

$$q_t = q_e (1 - e^{-k_1 t}) \quad (8)$$

$$\frac{t}{q_t} = \frac{1}{k_2 q_e^2} + \frac{1}{q_e} t \quad (9)$$

where  $q_t$  and  $Q_e$  (in mg P/L) are the adsorption capacities at time  $t$  (in min) and at equilibrium, respectively and  $K_1$  and  $K_2$  are the kinetic constants.

**4.7. Influence of Coexisting Ions on Adsorption Capacity.** KH<sub>2</sub>PO<sub>4</sub> (100 mg P/L) together with either KCl, K<sub>2</sub>CO<sub>3</sub>, KHCO<sub>3</sub>, KNO<sub>3</sub>, or K<sub>2</sub>SO<sub>4</sub> solution was mixed to obtain a 1:1 (by weight) ratio of the corresponding anions and P (that is, the concentration of each anion is 100 mg/L). Then, 0.05 g of the BC-5 sample was added. The adsorption process and phosphate determination are the same as those in Section 4.3. These five anions widely exist in natural water and affect the adsorption of phosphate by biochar. Therefore, we need to know the adsorption of biochar on phosphate when these anions are present in natural water.

**4.8. Characterization.** Sample surface morphologies were analyzed by field-emission scanning electron microscopy (FE-SEM) manufactured by Zeiss Giminer 300 (Germany) and coupled with X-ray energy-dispersive spectroscopy (EDS) (BC and BC-5). C, H, O, N, and S contents were determined by Elementar Vario EL cube instrument (Germany), while P, Ca, and K contents were analyzed by the inductively coupled plasma optical emission spectrometry (ICP-OES) performed using Agilent 725 instrument (sheep manure, oyster shell, BC, BC-5, and material of BC-5 after phosphate adsorption (BC-5 + P)). The surface area and porosity were obtained by Micromeritics ASAP2460 (sheep manure, BC, and BC-5). Fourier transform infrared (FTIR) spectra were recorded in the 4000–400 cm<sup>-1</sup> range using the Thermo Fisher Nicoletts 15 instrument (BC, BC-5, and BC-5 + P). X-ray diffraction (XRD) was performed by the Bruker D8 ADVANCE (Germany) instrument in the 5–85° 2θ range (BC, BC-5, and BC-5 + P). The data were processed using Jade 6.5 software.

## ■ AUTHOR INFORMATION

### Corresponding Author

Feng Wang – Agro-Environmental Protection Institute, Ministry of Agriculture and Rural Affairs, Tianjin 300191, China; Dali Agro-Environmental Science Station, Ministry of Agriculture and Rural Affairs, Dali 671004, China; Phone: +8613821305040; Email: wangfeng\_530@163.com

**Authors**

**Yiyang Feng** – Agro-Environmental Protection Institute, Ministry of Agriculture and Rural Affairs, Tianjin 300191, China; Dali Agro-Environmental Science Station, Ministry of Agriculture and Rural Affairs, Dali 671004, China;  
✉ [orcid.org/0000-0003-0528-3831](https://orcid.org/0000-0003-0528-3831)

**Di Zhao** – Agro-Environmental Protection Institute, Ministry of Agriculture and Rural Affairs, Tianjin 300191, China; Dali Agro-Environmental Science Station, Ministry of Agriculture and Rural Affairs, Dali 671004, China

**Shangkai Qiu** – Agro-Environmental Protection Institute, Ministry of Agriculture and Rural Affairs, Tianjin 300191, China; Dali Agro-Environmental Science Station, Ministry of Agriculture and Rural Affairs, Dali 671004, China

**Qiuping He** – Agro-Environmental Protection Institute, Ministry of Agriculture and Rural Affairs, Tianjin 300191, China; Dali Agro-Environmental Science Station, Ministry of Agriculture and Rural Affairs, Dali 671004, China

**Yuan Luo** – Agro-Environmental Protection Institute, Ministry of Agriculture and Rural Affairs, Tianjin 300191, China; Dali Agro-Environmental Science Station, Ministry of Agriculture and Rural Affairs, Dali 671004, China

**Keqiang Zhang** – Agro-Environmental Protection Institute, Ministry of Agriculture and Rural Affairs, Tianjin 300191, China; Dali Agro-Environmental Science Station, Ministry of Agriculture and Rural Affairs, Dali 671004, China;  
✉ [orcid.org/0000-0002-5791-7907](https://orcid.org/0000-0002-5791-7907)

**Shizhou Shen** – Agro-Environmental Protection Institute, Ministry of Agriculture and Rural Affairs, Tianjin 300191, China; Dali Agro-Environmental Science Station, Ministry of Agriculture and Rural Affairs, Dali 671004, China

Complete contact information is available at:

<https://pubs.acs.org/10.1021/acsomega.1c05191>

**Author Contributions**

Y.F. and D.Z. contributed equally to the work and should be regarded as co-first authors. Y.F.: conceptualization, methodology, data curation, formal analysis, and writing original draft; D.Z.: conceptualization, data curation, software, and investigation; S.Q.: methodology, data curation, and formal analysis; Q.H.: visualization and investigation; Y.L.: methodology and software; K.Z. and S.S.: writing—review and editing; and F.W.: funding acquisition, project administration, supervision, and writing—review and editing.

**Notes**

The authors declare no competing financial interest. The datasets generated and/or analyzed during the current study are available from the corresponding author on reasonable request.

**ACKNOWLEDGMENTS**

This work was financially supported by the National Key Research and Development Program of China (2017YFD0800403), the Central Public-Interest Scientific Institution Basal Research Fund (Y2021XC18), and the Yunnan Province Major Science and Technology Special Program (202102AE090011).

**REFERENCES**

- (1) Yuan, Z.; Ji, J.; Sheng, H.; Jiang, S.; Chen, T.; Liu, X.; Liu, X.; Zhuang, Y.; Zhang, L. Animal based diets and environment:

Perspective from phosphorus flow quantifications of livestock and poultry raising in China. *J. Environ. Manage.* **2019**, *244*, 199–207.

(2) Wu, H.; Zhang, Y.; Yuan, Z.; Gao, L. A review of phosphorus management through the food system: identifying the roadmap to ecological agriculture. *J. Cleaner Prod.* **2016**, *114*, 45–54.

(3) Ma, L.; Velthof, G. L.; Wang, F. H.; Qin, W.; Zhang, W. F.; Liu, Z.; Zhang, Y.; Wei, J.; Lesschen, J. P.; Ma, W. Q.; Oenema, O.; Zhang, F. S. Nitrogen and phosphorus use efficiencies and losses in the food chain in China at regional scales in 1980 and 2005. *Sci. Total Environ.* **2012**, *434*, 51–61.

(4) Sikder, S.; Joardar, J. C. Biochar production from poultry litter as management approach and effects on plant growth. *Int. J. Recycl. Org. Waste Agric.* **2018**, *8*, 47–58.

(5) Dunnigan, L.; Ashman, P. J.; Zhang, X.; Kwong, C. W. Production of biochar from rice husk: Particulate emissions from the combustion of raw pyrolysis volatiles. *J. Cleaner Prod.* **2018**, *172*, 1639–1645.

(6) Hosseini, S. H.; Liang, X.; Niyungeko, C.; Miaomiao, H.; Li, F.; Khan, S.; Eltohamy, K. M. Effect of sheep manure-derived biochar on colloidal phosphorus release in soils from various land uses. *Environ. Sci. Pollut. Res.* **2019**, *26*, 36367–36379.

(7) Chen, Q.; Qin, J.; Sun, P.; Cheng, Z.; Shen, G. Cow dung-derived engineered biochar for reclaiming phosphate from aqueous solution and its validation as slow-release fertilizer in soil-crop system. *J. Cleaner Prod.* **2018**, *172*, 2009–2018.

(8) Choi, Y.-K.; Jang, H. M.; Kan, E.; Wallace, A. R.; Sun, W. Adsorption of phosphate in water on a novel calcium hydroxide-coated dairy manure-derived biochar. *Environ. Eng. Res.* **2018**, *24*, 434–442.

(9) Wang, S.; Kong, L.; Long, J.; Su, M.; Diao, Z.; Chang, X.; Chen, D.; Song, G.; Shih, K. Adsorption of phosphorus by calcium-flour biochar: Isotherm, kinetic and transformation studies. *Chemosphere* **2018**, *195*, 666–672.

(10) Marshall, J. A.; Morton, B. J.; Muhlack, R.; Chittleborough, D.; Kwong, C. W. Recovery of phosphate from calcium-containing aqueous solutions resulting from biochar-induced calcium phosphate precipitation. *J. Cleaner Prod.* **2017**, *165*, 27–35.

(11) Oliveira, F. R.; Patel, A. K.; Jaisi, D. P.; Adhikari, S.; Lu, H.; Khanal, S. K. Environmental application of biochar: Current status and perspectives. *Bioresour. Technol.* **2017**, *246*, 110–122.

(12) Tan, X.; Liu, Y.; Zeng, G.; Wang, X.; Hu, X.; Gu, Y.; Yang, Z. Application of biochar for the removal of pollutants from aqueous solutions. *Chemosphere* **2015**, *125*, 70–85.

(13) Vikrant, K.; Kim, K. H.; Ok, Y. S.; Tsang, D. C. W.; Tsang, Y. F.; Giri, B. S.; Singh, R. S. Engineered/designer biochar for the removal of phosphate in water and wastewater. *Sci. Total Environ.* **2018**, *616–617*, 1242–1260.

(14) Liu, W. J.; Jiang, H.; Yu, H. Q. Development of Biochar-Based Functional Materials: Toward a Sustainable Platform Carbon Material. *Chem. Rev.* **2015**, *115*, 12251–12285.

(15) Yao, Y.; Gao, B.; Chen, J.; Zhang, M.; Inyang, M.; Li, Y.; Alva, A.; Yang, L. Engineered carbon (biochar) prepared by direct pyrolysis of Mg-accumulated tomato tissues: characterization and phosphate removal potential. *Bioresour. Technol.* **2013**, *138*, 8–13.

(16) Karunanithi, R.; Ok, Y. S.; Dharmarajan, R.; Ahmad, M.; Seshadri, B.; Bolan, N.; Naidu, R. Sorption, kinetics and thermodynamics of phosphate sorption onto soybean stover derived biochar. *Environ. Technol. Innovation* **2017**, *8*, 113–125.

(17) Deng, W.; Zhang, D.; Zheng, X.; Ye, X.; Niu, X.; Lin, Z.; Fu, M.; Zhou, S. Adsorption recovery of phosphate from waste streams by Ca/Mg-biochar synthesis from marble waste, calcium-rich sepiolite and bagasse. *J. Cleaner Prod.* **2021**, *288*, No. 125638.

(18) Mohammadi, R.; Hezarjaribi, M.; Ramasamy, D. L.; Sillanpää, M.; Pihlajamäki, A. Application of a novel biochar adsorbent and membrane to the selective separation of phosphate from phosphate-rich wastewaters. *Chem. Eng. J.* **2021**, *407*, No. 126494.

(19) Zheng, H.; Wang, Z.; Deng, X.; Zhao, J.; Luo, Y.; Novak, J.; Herbert, S.; Xing, B. Characteristics and nutrient values of biochars

- produced from giant reed at different temperatures. *Bioresour. Technol.* **2013**, *130*, 463–471.
- (20) Yao, Y.; Gao, B.; Chen, J.; Yang, L. Engineered biochar reclaiming phosphate from aqueous solutions: mechanisms and potential application as a slow-release fertilizer. *Environ. Sci. Technol.* **2013**, *47*, 8700–8708.
- (21) Zhao, X.; Li, H.; Chen, M.; Li, K.; Wang, B.; Xu, Z.; Cao, S.; Zhang, L.; Deng, H.; Lu, J. Strong-bonding calcium phosphate coatings on carbon/carbon composites by ultrasound-assisted anodic oxidation treatment and electrochemical deposition. *Appl. Surf. Sci.* **2012**, *258*, 5117–5125.
- (22) Novais, S. V.; Zenero, M. D. O.; Tronto, J.; Conz, R. F.; Cerri, C. E. P. Poultry manure and sugarcane straw biochars modified with MgCl<sub>2</sub> for phosphorus adsorption. *J. Environ. Manage.* **2018**, *214*, 36–44.
- (23) Zhang, M.; Gao, B.; Yao, Y.; Xue, Y.; Inyang, M. Synthesis of porous MgO-biochar nanocomposites for removal of phosphate and nitrate from aqueous solutions. *Chem. Eng. J.* **2012**, *210*, 26–32.
- (24) Cui, X.; Dai, X.; Khan, K. Y.; Li, T.; Yang, X.; He, Z. Removal of phosphate from aqueous solution using magnesium-alginate/chitosan modified biochar microspheres derived from Thalia dealbata. *Bioresour. Technol.* **2016**, *218*, 1123–1132.
- (25) Wu, L.; Zhang, S.; Wang, J.; Ding, X. Phosphorus retention using iron (II/III) modified biochar in saline-alkaline soils: Adsorption, column and field tests. *Environ. Pollut.* **2020**, *261*, No. 114223.
- (26) Jia, Z.; Zeng, W.; Xu, H.; Li, S.; Peng, Y. Adsorption removal and reuse of phosphate from wastewater using a novel adsorbent of lanthanum-modified platanus biochar. *Process Saf. Environ. Prot.* **2020**, *140*, 221–232.
- (27) Wang, Z.; Lin, Y.; Wu, D.; Kong, H. Hydrous iron oxide modified diatomite as an active filtration medium for phosphate capture. *Chemosphere* **2016**, *144*, 1290–1298.
- (28) Wu, Y.; Li, X.; Yang, Q.; Wang, D.; Xu, Q.; Yao, F.; Chen, F.; Tao, Z.; Huang, X. Hydrated lanthanum oxide-modified diatomite as highly efficient adsorbent for low-concentration phosphate removal from secondary effluents. *J. Environ. Manage.* **2019**, *231*, 370–379.
- (29) Ajmal, Z.; Muhammed, A.; Usman, M.; Kizito, S.; Lu, J.; Dong, R.; Wu, S. Phosphate removal from aqueous solution using iron oxides: Adsorption, desorption and regeneration characteristics. *J. Colloid Interface Sci.* **2018**, *528*, 145–155.
- (30) Saha, B.; Griffin, L.; Blunden, H. Adsorptive separation of phosphate oxyanion from aqueous solution using an inorganic adsorbent. *Environ. Geochem. Health* **2010**, *32*, 341–347.
- (31) Dai, L.; Tan, F.; Li, H.; Zhu, N.; He, M.; Zhu, Q.; Hu, G.; Wang, L.; Zhao, J. Calcium-rich biochar from the pyrolysis of crab shell for phosphorus removal. *J. Environ. Manage.* **2017**, *198*, 70–74.
- (32) Cao, H.; Wu, X.; Syed-Hassan, S. S. A.; Zhang, S.; Mood, S. H.; Milan, Y. J.; Garcia-Perez, M. Characteristics and mechanisms of phosphorous adsorption by rape straw-derived biochar functionalized with calcium from eggshell. *Bioresour. Technol.* **2020**, *318*, No. 124063.
- (33) Dalahmeh, S. S.; Stenström, Y.; Jebrane, M.; Hylander, L. D.; Daniel, G.; Heinmaa, I. Efficiency of Iron- and Calcium-Impregnated Biochar in Adsorbing Phosphate From Wastewater in Onsite Wastewater Treatment Systems. *Front. Environ. Sci.* **2020**, *8*, No. 538539.
- (34) Antunes, E.; Jacob, M. V.; Brodie, G.; Schneider, P. A. Isotherms, kinetics and mechanism analysis of phosphorus recovery from aqueous solution by calcium-rich biochar produced from biosolids via microwave pyrolysis. *J. Environ. Chem. Eng.* **2018**, *6*, 395–403.
- (35) Park, J. H.; Wang, J. J.; Xiao, R.; Zhou, B.; Delaune, R. D.; Seo, D. C. Effect of pyrolysis temperature on phosphate adsorption characteristics and mechanisms of crawfish char. *J. Colloid Interface Sci.* **2018**, *525*, 143–151.
- (36) Liu, X.; Shen, F.; Smith, R. L., Jr; Qi, X. Black liquor-derived calcium-activated biochar for recovery of phosphate from aqueous solutions. *Bioresour. Technol.* **2019**, *294*, No. 122198.
- (37) Yao, Y.; Gao, B.; Inyang, M.; Zimmerman, A. R.; Cao, X.; Pullammanappallil, P.; Yang, L. Removal of phosphate from aqueous solution by biochar derived from anaerobically digested sugar beet tailings. *J. Hazard. Mater.* **2011**, *190*, 501–507.
- (38) Saadat, S.; Raei, E.; Talebbeydokhti, N. Enhanced removal of phosphate from aqueous solutions using a modified sludge derived biochar: Comparative study of various modifying cations and RSM based optimization of pyrolysis parameters. *J. Environ. Manage.* **2018**, *225*, 75–83.
- (39) He, Q.; Luo, Y.; Feng, Y.; Xie, K.; Zhang, K.; Shen, S.; Luo, Y.; Wang, F. Biochar produced from tobacco stalks, eggshells, and Mg for phosphate adsorption from a wide range of pH aqueous solutions. *Mater. Res. Express* **2020**, *7*, No. 115603.
- (40) Notodarmojo, P. A.; Fujiwara, T.; Habuer; Pham Van, D. Effectiveness of oyster shell as alkali additive for two-stage anaerobic co-digestion: Carbon flow analysis. *Energy* **2022**, *239*, No. 122177.
- (41) H Silva, T.; Mesquita-Guimarães, J.; Henriques, B.; Silva, F. S.; Fredel, M. C. The Potential Use of Oyster Shell Waste in New Value-Added By-Product. *Resources* **2019**, *8*, No. 13.
- (42) Luo, Y.; Xie, K.; Feng, Y.; He, Q.; Zhang, K.; Shen, S.; Wang, F. Synthesis of a La(OH)<sub>3</sub> nanorod/walnut shell biochar composite for reclaiming phosphate from aqueous solutions. *Colloids Surf., A* **2021**, *610*, No. 125736.
- (43) Liu, S.-b.; Tan, X.-f.; Liu, Y.-g.; Gu, Y.-l.; Zeng, G.-m.; Hu, X.-j.; Wang, H.; Zhou, L.; Jiang, L.-h.; Zhao, B.-b. Production of biochars from Ca impregnated ramie biomass (*Boehmeria nivea* (L.) Gaud.) and their phosphate removal potential. *RSC Adv.* **2016**, *6*, 5871–5880.
- (44) Feng, Y.; Luo, Y.; He, Q.; Zhao, D.; Zhang, K.; Shen, S.; Wang, F. Performance and mechanism of a biochar-based Ca-La composite for the adsorption of phosphate from water. *J. Environ. Chem. Eng.* **2021**, *9*, No. 105267.
- (45) Fang, C.; Zhang, T.; Li, P.; Jiang, R.; Wu, S.; Nie, H.; Wang, Y. Phosphorus recovery from biogas fermentation liquid by Ca-Mg loaded biochar. *J. Environ. Sci.* **2015**, *29*, 106–14.
- (46) Yin, H.; Kong, M.; Fan, C. Batch investigations on P immobilization from wastewaters and sediment using natural calcium rich sepiolite as a reactive material. *Water. Res.* **2013**, *47*, 4247–4258.
- (47) Perassi, I.; Borgnino, L. Adsorption and surface precipitation of phosphate onto CaCO<sub>3</sub>–montmorillonite: effect of pH, ionic strength and competition with humic acid. *Geoderma* **2014**, *232–234*, 600–608.
- (48) Mitrogiannis, D.; Psychoyou, M.; Baziotis, I.; Inglezakis, V. J.; Koukouzas, N.; Tsoukalas, N.; Palles, D.; Kamitsos, E.; Oikonomou, G.; Markou, G. Removal of phosphate from aqueous solutions by adsorption onto Ca(OH)<sub>2</sub> treated natural clinoptilolite. *Chem. Eng. J.* **2017**, *320*, 510–522.
- (49) Hermassi, M.; Valderrama, C.; Moreno, N.; Font, O.; Querol, X.; Batis, N.; Cortina, J. L. Powdered Ca-activated zeolite for phosphate removal from treated waste-water. *J. Chem. Technol. Biotechnol.* **2016**, *91*, 1962–1971.
- (50) Yin, H.; Han, M.; Tang, W. Phosphorus sorption and supply from eutrophic lake sediment amended with thermally-treated calcium-rich attapulgite and a safety evaluation. *Chem. Eng. J.* **2016**, *285*, 671–678.
- (51) Dai, L.; Wu, B.; Tan, F.; He, M.; Wang, W.; Qin, H.; Tang, X.; Zhu, Q.; Pan, K.; Hu, Q. Engineered hydrochar composites for phosphorus removal/recovery: Lanthanum doped hydrochar prepared by hydrothermal carbonization of lanthanum pretreated rice straw. *Bioresour. Technol.* **2014**, *161*, 327–332.
- (52) Wang, Z.; Guo, H.; Shen, F.; Yang, G.; Zhang, Y.; Zeng, Y.; Wang, L.; Xiao, H.; Deng, S. Biochar produced from oak sawdust by Lanthanum (La)-involved pyrolysis for adsorption of ammonium (NH<sub>4</sub><sup>+</sup>), nitrate (NO<sub>3</sub><sup>-</sup>), and phosphate (PO<sub>4</sub><sup>3-</sup>). *Chemosphere* **2015**, *119*, 646–653.
- (53) Rashid, M.; Price, N. T.; Gracia Pinilla, M. A.; O'Shea, K. E. Effective removal of phosphate from aqueous solution using humic acid coated magnetite nanoparticles. *Water. Res.* **2017**, *123*, 353–360.

(54) Yang, F.; Zhang, S.; Sun, Y.; Tsang, D. C. W.; Cheng, K.; Ok, Y. S. Assembling biochar with various layered double hydroxides for enhancement of phosphorus recovery. *J. Hazard. Mater.* **2019**, *365*, 665–673.